

On the Finite-Sample Performance of Measure Transportation-Based Multivariate Rank Tests

Marc Hallin and Gilles Mordant

Abstract Extending to dimension 2 and higher the dual univariate concepts of ranks and quantiles has remained an open problem for more than half a century. Based on measure transportation results, a solution has been proposed recently under the name *center-outward ranks and quantiles* which, contrary to previous proposals, enjoys all the properties that make univariate ranks a successful tool for statistical inference. Just as their univariate counterparts (to which they reduce in dimension one), center-outward ranks allow for the construction of distribution-free and asymptotically efficient tests for a variety of problems where the density of some noise or innovation remains unspecified. The actual implementation of these tests involves the somewhat arbitrary choice of a grid. While the asymptotic impact of that choice is nil, its finite-sample consequences are not. In this note, we investigate the finite-sample impact of that choice in the typical context of the multivariate two-sample location problem.

1 Introduction

1.1 David Tyler, beyond affine equivariance and elliptical symmetry

The closely related concepts of affine equivariance and elliptical symmetry played a central role in the development of robust multivariate statistics over the past 60

Marc Hallin
ECARES and Département de Mathématique, Université libre de Bruxelles, Avenue F.D. Roosevelt 50, 1050 Brussels, Belgium
e-mail: mhallin@ulb.ac.be

Gilles Mordant
IMS, Universität Göttingen, Goldschmidtstraße 7, 37077 Göttingen, Germany
e-mail: mordantgilles@gmail.com

years.¹ A critical attitude towards this dominant role of elliptical densities constitutes a red thread running through all of David's contributions to multivariate analysis²—an attitude that actually takes place in a broader debate on the ordering of the real space in dimension $d \geq 2$. Such ordering is an essential issue if the univariate concepts of distribution and quantile functions, ranks, and signs, all heavily depending on the canonical ordering of the real line, are to be extended to a multivariate context.

1.2 Ordering the real space in dimension $d \geq 2$

The problem of ordering \mathbb{R}^d for $d \geq 2$, hence ranking multivariate observations, has a long history in statistics. Many attempts have been made to define adequate multivariate concepts of ranks.

The notion of ranks, however, is not an isolated one, as it is inseparable from that of empirical quantiles, quantile regions (collections of points with ranks less than or equal to some given value), and quantile contours (collections of points with ranks equal to some given value). A sound definition thus should include all these concepts, along with their population versions—the population distribution and quantile functions F and Q —and their mutual relations (a quantile function is the inverse of a distribution function ($Q = F^{-1}$); a population distribution function and its empirical version are asymptotically related via a Glivenko-Cantelli result, etc.). Among the key properties of any successful concept are the distribution-freeness (within the class of absolutely continuous distributions P , say) of the ranks and the distribution-freeness of the push-forward³ of a distribution P by its distribution function F . Without these distribution-freeness properties, the level of a quantile $Q(\tau) = F^{-1}(\tau)$ depends on the distribution P characterized by F and can be anything larger or smaller than τ : as a quantile of order τ , thus, $Q(\tau)$ is totally meaningless.

Appealing as they are, none of the attempts that had been made until recently—marginal ranks, spatial ranks, elliptical (or Mahalanobis) ranks, ... —is satisfying the desired properties; actually, none of them is even enjoying distribution-freeness!⁴ Nor do the various depth concepts: the probability content of a depth contour of given depth strongly depends on the underlying P , which hinders its interpretation as a quantile contour.

Based on measure transportation results (mainly, a theorem by McCann (1995)) Chernozhukov et al. (2017), Hallin (2017), and Hallin et al. (2021) recently intro-

¹ Tukey (1960), Huber (1964), and Hampel (1968) generally are considered as laying the foundations of modern robust statistics; see Ronchetti (2006) for a historical perspective and Stigler (1973) for an account of the pre-Tukey era.

² Significantly, “*Robust Multivariate Statistics: Beyond Ellipticity and Affine Equivariance*” is the title of one of David's NSF grants.

³ We adopt here the convenient terminology and notation of measure transportation: the push-forward $F\#P$ of P by F is the distribution of $F(Z)$ where $Z \sim P$, i.e., $F(Z) \sim F\#P$ if $Z \sim P$.

⁴ The Mahalanobis ranks and signs (Hallin & Paindaveine, 2002) are enjoying distribution-freeness over the class of elliptically symmetric distributions only.

duced the concepts of *center-outward ranks* and *signs, distribution* and *quantile functions* which, for the first time, satisfy all the desired properties (see Hallin et al. (2021) and the review by Hallin (2022) for details) and further triggered the development of several appealing multivariate, distribution-free statistical procedures, among which Faugeras & Rüschendorf (2017), Shi et al. (2021a,b), Ghosal & Sen (2019), Deb & Sen (2021), Deb et al. (2020, 2021), Masud & Aeron (2021), Hallin et al. (2020a,b,c). These are the concepts we are considering in this paper and now describe under their various versions.

2 Center-outward ranks and signs

For the simplicity of exposition, we throughout consider distributions P on \mathbb{R}^d in the family \mathcal{P}^d of Lebesgue-absolutely continuous distributions with *nonvanishing densities*, that is, with a density f such that for all $B > 0$ there exist $0 < m_B^- \leq m_B^+ < \infty$ such that $m_B^- \leq f(\mathbf{z}) \leq m_B^+$ for all \mathbf{z} such that $\|\mathbf{z}\| \leq B$. That assumption can be relaxed, though: see del Barrio et al. (2020).

2.1 A measure transportation-based concept of distribution and quantile functions

The basic idea behind the definition of the center-outward distribution and quantile functions of a probability measure $P \in \mathcal{P}^d$ is quite simple. For $d = 1$, the distribution function F of P is the unique monotone increasing function pushing P forward to the uniform $U_{[0,1]}$ over $[0, 1]$ —namely, $F\#P = U_{[0,1]}$. Rather than F , however, which is based on a left-to-right ordering of \mathbb{R} that does not extend to \mathbb{R}^d for $d \geq 2$, we consider the *center-outward distribution function* $F_\pm := 2F - 1$, which contains the same information as F and is the unique monotone increasing function pushing P forward to the uniform $U_{[-1,1]}$ over $[-1, 1]$. A monotone increasing function is the gradient (the derivative) of a convex function: the center-outward distribution function F_\pm this is the unique gradient of a convex function such that $F_\pm\#P = U_{[-1,1]}$. The interval $[-1, 1]$ is, for $d = 1$, the closed unit ball $\bar{\mathbb{S}}_d$, where $\mathbb{S}_d := \{\mathbf{u} \mid \|\mathbf{u}\| \leq 1\}$ and, denoting by U_d the spherical uniform⁵ over $\bar{\mathbb{S}}_d$, the spherical uniform over $\bar{\mathbb{S}}_1$ coincides with the uniform over $[-1, 1]$: namely, $U_1 = U_{[-1,1]}$.

A celebrated theorem by McCann (1995) tells us that, for arbitrary dimension $d \in \mathbb{N}$ and arbitrary $P \in \mathcal{P}^d$, there exist a (P -a.s., here Lebesgue-a.e.) unique gradient of a convex function \mathbf{F}_\pm such that $\mathbf{F}_\pm\#P = U_d$. Obviously, for $d = 1$, \mathbf{F}_\pm coincides with the univariate F_\pm , whence the notation. Call \mathbf{F}_\pm the *center-outward distribution function* of P . It follows from Figalli (2018) that—except perhaps at $\mathbf{F}_\pm^{-1}(\mathbf{0})$

⁵ The *spherical uniform* U_d over $\bar{\mathbb{S}}_d$ is the spherical distribution with center $\mathbf{0}$ and radial density the uniform over $[0, 1]$: it is thus the product of a uniform over $[0, 1]$ for the distances to the origin and a uniform over the unit (hyper)sphere for the directions.

(a set of points with Lebesgue measure zero)— $\mathbf{F}_\pm \# \mathbf{P}$ is a homeomorphism, hence admits a continuous (except perhaps at $\mathbf{F}_\pm^{-1}(\mathbf{0})$) inverse $\mathbf{Q}_\pm := \mathbf{F}_\pm^{-1}$: call \mathbf{Q}_\pm the *center-outward quantile function* of \mathbf{P} . Clearly, $\mathbf{Q}_\pm \# \mathbf{U}_d = \mathbf{P}$.

This, with the spherical uniform \mathbf{U}_d as a reference distribution (extending $\mathbf{U}_{[-1,1]}$) is the concept proposed in Hallin (2017) and Hallin et al. (2021), where we refer to for further properties of \mathbf{F}_\pm and \mathbf{Q}_\pm justifying their qualification as distribution and quantile functions.

Other choices are possible for the reference \mathbf{U} , though. Replacing \mathbf{U}_d with an arbitrary compactly supported absolutely continuous reference distribution \mathbf{U} , Chernozhukov et al. (2017), in a very general approach, propose, under the name of *Monge-Kantorovich vector rank* and *Monge-Kantorovich quantile functions*, measure transportation-based definitions of a broad class of analogues, \mathbf{F}_{MK} and \mathbf{Q}_{MK} , say, of \mathbf{F}_\pm and \mathbf{Q}_\pm . For nonspherical \mathbf{U} 's, however, the Monge-Kantorovich quantile functions do not enjoy all the features expected from a quantile function;⁶ Chernozhukov et al. (2017) therefore also introduce a concept of *Monge-Kantorovich depth* D_{MK} —a transformation-retransformation version (based on the Monge-Kantorovich vector rank function) of classical Tukey depth D_{Tukey} . For spherical \mathbf{U} 's, Monge-Kantorovich depth and quantile contours coincide. More precisely, defining $\delta(\tau) := D_{\text{Tukey}}(\mathbf{u}_\tau)$ where \mathbf{u}_τ is such that $\mathbf{U}(\{\mathbf{u} \mid \|\mathbf{u}\| \leq \|\mathbf{u}_\tau\|\}) = \tau$, one has $\{\mathbf{z} \mid \|\mathbf{F}_{\text{MK}}\| = \tau\} = D_{\text{MK}}^{-1}(\delta(\tau))$. Recurring to depth in order to construct quantile regions and contours, thus, is not necessary in the case of a spherical reference \mathbf{U} which, in that respect, offers a better conceptual coherence between the resulting notions of vector ranks and quantiles. As far as rank tests are concerned, however, this can be considered a minor concern.

The choice for \mathbf{U} of the nonspherical Lebesgue uniform $\mathbf{U}_{[0,1]^d}$ over the unit (in the canonical basis) hypercube $[0, 1]^d$ —call it the *cubic uniform*—yields a vector rank function \mathbf{F}_{MK} that reduces, for $d = 1$, to the classical distribution function F just as \mathbf{F}_\pm reduces to F_\pm . Despite poor equivariance properties⁷ its use has been advocated by several authors: see, e.g., Faugeras & Rüschendorf (2017), Carlier et al. (2016), Deb et al. (2020, 2021), Deb & Sen (2021).

2.2 Multivariate ranks and signs

Denote by $\mathbf{Z}^{(n)} := (\mathbf{Z}_1^{(n)}, \dots, \mathbf{Z}_n^{(n)})$ an i.i.d. sample with distribution $\mathbf{P} \in \mathcal{P}^d$. The empirical counterpart $\mathbf{F}_\pm^{(n)}$ of \mathbf{F}_\pm is obtained as the solution of an optimal pairing problem between the sample values $\mathbf{Z}_1^{(n)}, \dots, \mathbf{Z}_n^{(n)}$ and a “regular” grid $\mathfrak{G}^{(n)}$ with gridpoints $\mathfrak{G}_1^{(n)}, \dots, \mathfrak{G}_n^{(n)}$. Precisely, $(\mathbf{F}_\pm^{(n)}(\mathbf{Z}_1^{(n)}), \dots, \mathbf{F}_\pm^{(n)}(\mathbf{Z}_n^{(n)}))$ is defined as the

⁶ On this point, see Section 3.4 in Hallin (2022).

⁷ Contrary to \mathbf{F}_\pm , which is nicely equivariant, the rank vector function \mathbf{F}_{MK} associated with the cubic uniform $\mathbf{U}_{[0,1]^d}$ is highly non-equivariant under orthogonal transformations.

minimizer $(\mathfrak{G}_{\pi^*(1)}^{(n)}, \dots, \mathfrak{G}_{\pi^*(n)}^{(n)})$, over the $n!$ possible permutations $\pi \in \Pi_n$ of the integers $\{1, \dots, n\}$, of $\sum_{i=1}^n \|\mathbf{Z}_i^{(n)} - \mathfrak{G}_{\pi(i)}^{(n)}\|^2$.

The choice of the grid $\mathfrak{G}^{(n)}$, of course, depends on the reference distribution U adopted in the definitions of Section 2.1: in particular, the uniform discrete distribution over the n gridpoints $\mathfrak{G}_1^{(n)}, \dots, \mathfrak{G}_n^{(n)}$ should converge weakly to U as $n \rightarrow \infty$. Our objective is to investigate the finite-sample performance of two-sample location tests based on

- (Ti) the empirical center-outward distribution function $\mathbf{F}_{\pm}^{(n)}$ associated with the spherical uniform reference distribution $U = U_d$;
- (Tii) the empirical Monge-Kantorovich vector ranks $\mathbf{F}_{\square}^{(n)}$ associated with the cubic uniform reference distribution $U = U_{[0,1]^d}$;
- (Tiii) the empirical Monge-Kantorovich vector ranks $\mathbf{F}_{\pm \mathcal{N}}^{(n)}$ associated with the Gaussian $\mathcal{N}(\mathbf{0}, \mathbf{I}_d)$ reference considered as a spherical distribution;
- (Tiv) the empirical Monge-Kantorovich vector ranks $\mathbf{F}_{\square \mathcal{N}}^{(n)}$ associated with the Gaussian $\mathcal{N}(\mathbf{0}, \mathbf{I}_d)$ reference considered as a product of univariate standard normal distributions.

The grids we are using for these four cases are constructed as follows (see Section 3.1 for details on Halton sequences and the choice of n_R and n_S):

- (Gi) $U = U_d$: (a) factorize n into $n = n_R n_S + n_0$ with $n_0 < \min(n_R, n_S)$; (b) generate a Halton sequence $\mathfrak{S}_{(n_S)} := (\mathbf{u}_1, \dots, \mathbf{u}_{n_S})$ over the unit (hyper)sphere \mathcal{S}_{d-1} ; (c) the grid $\mathfrak{G}^{(n)}$ consists of the intersections of these n_S unit vectors with the n_R hyperspheres centered at $\mathbf{0}$, with radii $j/(n_R + 1)$, $j = 1, \dots, n_R$ —along with n_0 copies of the origin;
- (Gii) $U = U_{[0,1]^d}$: the grid $\mathfrak{G}^{(n)}$ is a Halton sequence over $[0, 1]^d$;
- (Giii) $U = \mathcal{N}(\mathbf{0}, \mathbf{I}_d)$, spherical grid: the grid $\mathfrak{G}^{(n)}$ is the image, by the radial transformation $\mathbf{z} \mapsto \sqrt{F_{\chi_d^2}^{-1}(\|\mathbf{z}\|)} \mathbf{z}$, of the spherical grid constructed in (i), where $F_{\chi_d^2}$ denotes the chi-square distribution function with d degrees of freedom;
- (Giv) $U = \mathcal{N}(\mathbf{0}, \mathbf{I}_d)$, cubic grid: the grid $\mathfrak{G}^{(n)}$ is the image, by componentwise application of the standard normal quantile transformation $z_i \mapsto \Phi^{-1}(z_i)$,⁸ of a Halton sequence over $[0, 1]^d$.

Remark 1 The grid $\mathfrak{G}^{(n)}$ in (Gi) reduces, for $d = 1$, to

$$\{\pm 1/(\lceil n/2 \rceil + 1), \dots, \pm \lceil n/2 \rceil/(\lceil n/2 \rceil + 1)\}$$

along with the origin in case n is odd; that grid is of the form

$$\{2(1/(n+1)) - 1, \dots, 2(n/(n+1)) - 1\}$$

where $\{1/(n+1), \dots, n/(n+1)\}$ is the grid producing traditional univariate ranks to which the grid $\mathfrak{G}^{(n)}$ in (Gii) also reduces for $d = 1$.

⁸ As usual, we denote by Φ the standard normal distribution function, by Φ^{-1} the standard normal quantile function.

Remark 2 In (Gi) and (Giii), the grid $\mathfrak{G}^{(n)}$ is spherical; as a consequence, $\mathbf{F}_{\pm}^{(n)}(\mathbf{Z}_i^{(n)})$ and $\mathbf{F}_{\pm\mathcal{N}}^{(n)}(\mathbf{Z}_i^{(n)})$ in (Ti) and (Tiii) naturally factorize as

$$\mathbf{F}_{\pm}^{(n)}(\mathbf{Z}_i^{(n)}) = \|\mathbf{F}_{\pm}^{(n)}(\mathbf{Z}_i^{(n)})\| \frac{\mathbf{F}_{\pm}^{(n)}(\mathbf{Z}_i^{(n)})}{\|\mathbf{F}_{\pm}^{(n)}(\mathbf{Z}_i^{(n)})\|} =: \frac{R_{i\pm}^{(n)}}{n_R + 1} \mathbf{S}_{i\pm}^{(n)}$$

where $R_{i\pm}^{(n)} = (n_R + 1)\|\mathbf{F}_{\pm}^{(n)}(\mathbf{Z}_i^{(n)})\|$, ranging from 0 or 1 (according as $n_0 \neq 0$ or $n_0 = 0$) to n_R , is the *center-outward rank* of $\mathbf{Z}_i^{(n)}$ and $\mathbf{S}_{i\pm}^{(n)}$ (a unit vector) has the interpretation of a (multivariate) *center-outward sign* and

$$\mathbf{F}_{\pm\mathcal{N}}^{(n)}(\mathbf{Z}_i^{(n)}) = \|\mathbf{F}_{\pm\mathcal{N}}^{(n)}(\mathbf{Z}_i^{(n)})\| \frac{\mathbf{F}_{\pm\mathcal{N}}^{(n)}(\mathbf{Z}_i^{(n)})}{\|\mathbf{F}_{\pm\mathcal{N}}^{(n)}(\mathbf{Z}_i^{(n)})\|} =: J_{\text{vdW}} \left(\frac{R_{i\pm\mathcal{N}}^{(n)}}{n_R + 1} \right) \mathbf{S}_{i\pm\mathcal{N}}^{(n)} \quad (1)$$

where $J_{\text{vdW}} = \sqrt{\frac{F^{-1}}{\chi_d^2}}$ is the univariate *normal* or *van der Waerden score function*, $R_{i\pm\mathcal{N}}^{(n)}$ the rank of $\|\mathbf{F}_{\pm\mathcal{N}}^{(n)}(\mathbf{Z}_i^{(n)})\|$ among the n_R distinct values of $\|\mathbf{F}_{\pm\mathcal{N}}^{(n)}(\mathbf{Z}_i^{(n)})\|$ for $i = 1, \dots, n$ and $\mathbf{S}_{i\pm\mathcal{N}}^{(n)}$ similarly has the interpretation of a multivariate sign. Being based on different transport maps, however, neither $R_{i\pm}^{(n)}$ and $R_{i\pm\mathcal{N}}^{(n)}$ nor $\mathbf{S}_{i\pm}^{(n)}$ and $\mathbf{S}_{i\pm\mathcal{N}}^{(n)}$ need coincide.

Remark 3 No similar factorization into ranks and signs occurs with the vector ranks $\mathbf{F}_{\square}^{(n)}$ and $\mathbf{F}_{\square\mathcal{N}}^{(n)}$ in (Tii) and (Tiv).

2.3 Distribution-free tests based on center-outward ranks and signs

Hallin et al. (2020a) propose, for multiple-output regression models with unspecified noise distribution $\mathbf{P} \in \mathcal{P}^d$, fully distribution-free yet, for adequate choice of scores, parametrically efficient center-outward rank tests of the null hypothesis of no-treatment effect based on the empirical center-outward distribution functions $\mathbf{F}_{\pm}^{(n)}$ (hence, the center-outward ranks and signs).

The particular case of two-sample location is treated by Deb et al. (2021) who also consider tests based on the empirical Monge-Kantorovich vector ranks $\mathbf{F}_{\text{MK}}^{(n)}$ associated with various reference distributions.

2.3.1 Score functions

In line with the classical theory developed, e.g., by Hájek & Šidák (1967), rank-based statistics, irrespective of the reference distribution, involve *score functions* or *scores*. Depending on the context, a score function is a mapping \mathbf{J} from the unit ball \mathbb{S}_d or the unit cube $[0, 1]^d$ to \mathbb{R}^d satisfying some mild regularity assumptions (continuity, square integrability, etc.: see, e.g. Hallin et al. (2020a), Assumption 3.1). The only score functions we are considering here are the *Wilcoxon*, the *spherical van der*

Waerden, and the *marginal van der Waerden score functions*

$$\mathbf{J}_W(\mathbf{u}) := \mathbf{u}, \quad \mathbf{J}_{\text{vdW}}^\pm(\mathbf{u}) := \sqrt{F_{\chi_d^2}^{-1}(\|\mathbf{u}\|)} \frac{\mathbf{u}}{\|\mathbf{u}\|}, \quad \text{and } \mathbf{J}_{\text{vdW}}^\square(\mathbf{u}) := \left(\Phi^{-1}(u_1), \dots, \Phi^{-1}(u_d) \right),$$

where $F_{\chi_d^2}$ and Φ stand for the (univariate) chi-square (d degrees of freedom) and standard normal distribution functions, respectively.

2.3.2 Test statistics

For simplicity, our investigation here is limited to that particular case of two-sample location models, where the n observations are i.i.d. under the null and consist of two samples, $\mathbf{Z}_1^{(n)}, \dots, \mathbf{Z}_{n_1}^{(n)}$ and $\mathbf{Z}_{n_1+1}^{(n)}, \dots, \mathbf{Z}_{n_1+n_2}^{(n)}$, with $n_1 + n_2 = n$. The classical procedure for this problem is Hotelling's test, based on a quadratic statistic of the form

$$\left(T_{\text{Hot}}^{(n)} \right)^2 = \Delta_{\text{Hot}}^{(n)'} \left(\Sigma_{\text{Hot}}^{(n)} \right)^{-1} \Delta_{\text{Hot}}^{(n)}$$

where $\Sigma_{\text{Hot}}^{(n)}$ is the estimated (under the null) covariance matrix of

$$\Delta_{\text{Hot}}^{(n)} := \frac{1}{n_1} \sum_{i=1}^{n_1} \mathbf{Z}_i^{(n)} - \frac{1}{n_2} \sum_{i=n_1+1}^n \mathbf{Z}_i^{(n)}.$$

The Hotelling test is parametrically efficient under Gaussian assumptions; it remains asymptotically valid,⁹ however, under mild moment assumptions and therefore qualifies as a pseudo-Gaussian procedure.

For score functions \mathbf{J} , the center-outward rank-based test statistics in Section 5.3.1 of Hallin et al. (2020a) are of the form

$$\left(\tilde{T}_{\mathbf{J}\pm}^{(n)} \right)^2 = \tilde{\Delta}_{\mathbf{J}\pm}^{(n)'} \left(\Sigma_{\mathbf{J}\pm} \right)^{-1} \tilde{\Delta}_{\mathbf{J}\pm}^{(n)} \quad (2)$$

where $\Sigma_{\mathbf{J}}$ is the exact or asymptotic covariance of

$$\tilde{\Delta}_{\mathbf{J}\pm}^{(n)} := \frac{1}{n_1} \sum_{i=1}^{n_1} \mathbf{J}(\mathbf{F}_{\pm}^{(n)}(\mathbf{Z}_i^{(n)})) - \frac{1}{n_2} \sum_{i=n_1+1}^n \mathbf{J}(\mathbf{F}_{\pm}^{(n)}(\mathbf{Z}_i^{(n)})). \quad (3)$$

Since the quadratic form (2) is invariant under affine transformations of $\tilde{\Delta}_{\mathbf{J}\pm}^{(n)}$ and since the sum $\sum_{i=1}^n \mathbf{J}(\mathbf{F}_{\pm}^{(n)}(\mathbf{Z}_i^{(n)}))$ is a deterministic constant that only depends on \mathbf{J} and the grid used in the definition of $\mathbf{F}_{\pm}^{(n)}$, the same test statistic can be based on

⁹ Asymptotically valid, here, means pointwise (with respect to the actual density of the observations) asymptotically correct nominal probability levels, not *uniformly* asymptotically correct nominal probability levels.

$$\Delta_{\mathbf{J}}^{(n)} = \frac{1}{n_1} \sum_{i=1}^{n_1} \mathbf{J}(\mathbf{F}_{\pm}^{(n)}(\mathbf{Z}_i^{(n)})) - \frac{1}{n} \sum_{i=1}^n \mathbf{J}(\mathbf{F}_{\pm}^{(n)}(\mathbf{Z}_i^{(n)})),$$

yielding the test statistic described in Section 5.3.1 of Hallin et al. (2020a) which, in the particular case of Wilcoxon and van der Waerden scores \mathbf{J}_W and \mathbf{J}_{vDW}^{\pm} , we denote as $\left(\tilde{T}_{W\pm}^{(n)}\right)^2$ and $\left(\tilde{T}_{vDW\pm}^{(n)}\right)^2$, respectively.

For the same testing problem, Deb et al. (2021) consider statistics of the form (2), but also

- (a) based on the empirical Monge-Kantorovich vector ranks $\mathbf{F}_{\square}^{(n)}$ associated with the cubic uniform reference $U = U_{[0,1]^d}$, statistics $T_{\mathbf{J}\square}^{(n)}$ and $\Delta_{\mathbf{J}\square}^{(n)}$ of the same form as $T_{\mathbf{J}\pm}^{(n)}$ and $\Delta_{\mathbf{J}\pm}^{(n)}$ in (2) and (3) but with $\mathbf{J}(\mathbf{F}_{\square}^{(n)}(\mathbf{Z}_i^{(n)}))$ substituting $\mathbf{J}(\mathbf{F}_{\pm}^{(n)}(\mathbf{Z}_i^{(n)}))$; denote by $\left(\tilde{T}_{W\square}^{(n)}\right)^2$ and $\left(\tilde{T}_{vDW\square}^{(n)}\right)^2$ the particular cases of the Wilcoxon and cubic van der Waerden statistics obtained for the scores \mathbf{J}_W and \mathbf{J}_{vDW}^{\pm} , respectively;
- (b) based on the empirical Monge-Kantorovich vector ranks $\mathbf{F}_{\pm\mathcal{N}}^{(n)}$ and $\mathbf{F}_{\square\mathcal{N}}^{(n)}$ associated with the spherical Gaussian reference $\mathcal{N}(\mathbf{0}, \mathbf{I}_d)$ considered as spherical or as a product of independent uniforms, statistics $T_{\mathbf{J}\pm\mathcal{N}}^{(n)}$ and $T_{\mathbf{J}\square\mathcal{N}}^{(n)}$ of the same form as $T_{\mathbf{J}\pm}^{(n)}$ and $\Delta_{\mathbf{J}\pm}^{(n)}$ in (2) and (3) but with $\mathbf{J}(\mathbf{F}_{\pm\mathcal{N}}^{(n)}(\mathbf{Z}_i^{(n)}))$ and $\mathbf{J}(\mathbf{F}_{\square\mathcal{N}}^{(n)}(\mathbf{Z}_i^{(n)}))$, respectively, substituting $\mathbf{J}(\mathbf{F}_{\pm}^{(n)}(\mathbf{Z}_i^{(n)}))$; this, for Wilcoxon scores $\mathbf{J}(\mathbf{u}) = \mathbf{u}$, yields the van der Waerden statistics $\left(\tilde{T}_{vDW\pm\mathcal{N}}^{(n)}\right)^2$ and $\left(\tilde{T}_{vDW\square\mathcal{N}}^{(n)}\right)^2$.

Remark 4 Although they are based on Wilcoxon (identity) scores, the terminology “van der Waerden statistic” for $\tilde{T}_{vDW\pm\mathcal{N}}^{(n)}$ and $\tilde{T}_{vDW\square\mathcal{N}}^{(n)}$ seems more appropriate than the terminology “Wilcoxon statistic” used by Deb et al. (2021), and is in line with the traditional terminology of rank-based inference. Both $\tilde{T}_{vDW\pm}^{(n)}$ and $\tilde{T}_{vDW\pm\mathcal{N}}^{(n)}$ indeed result from a transport from the sample values to a grid of Gaussian quantiles of the form (6iii). For $\tilde{T}_{vDW\pm}^{(n)}$, the transport is $\mathbf{J} \circ \mathbf{F}_{\pm}^{(n)}$, which, as a rule, is not an optimal one (not the gradient of a convex function) while, for $\tilde{T}_{vDW\pm\mathcal{N}}^{(n)}$, the transport is the optimal one $\mathbf{F}_{\pm\mathcal{N}}^{(n)}$; the difference between $\tilde{T}_{vDW\pm}^{(n)}$ and $\tilde{T}_{vDW\pm\mathcal{N}}^{(n)}$ thus essentially consists in the way the transport to the spherical Gaussian grid is performed. A similar remark can be made for $\tilde{T}_{vDW\square}^{(n)}$ and $\tilde{T}_{vDW\square\mathcal{N}}^{(n)}$.

3 Finite-sample performance: two-sample location simulations

It clearly appears that choices are to be made before performing a rank test based on the concepts of multivariate ranks developed on the previous sections: center-outward ranks? vector ranks? which ones? with which scores? The analysis of asymptotic performance does not help much, as the same local powers can be achieved by several alternatives. The objective of this paper is to determine whether finite-sample performance can help us with these choices. We restrict ourselves to the two-sample

location problem, Wilcoxon and van der Waerden scores, but the conclusions are quite likely to hold for the general case of multiple-output linear models considered in Hallin et al. (2020a).

Before explaining how simulations were conducted, let us provide some details on the way the grids described in Section 2.2 were constructed. Recall that the aim of these grids is to provide a discrete approximation of the chosen continuous reference distribution.

3.1 Halton sequences on the cube and the sphere ((Gii) and (Giv) grids)

The grid constructions (Gii) and (Giv) involve Halton sequences on the hypercube $[0, 1]^d$. Halton sequences are pseudo-random numbers with low discrepancy of classical use in methods such as Monte Carlo simulations. We used the implementation available in the package SDraw by McDonald & McDonald (2020). The grid construction in (Gi), hence also in (Giii), requires a n_S -point “Halton sequence” over the hypersphere \mathcal{S}^{d-1} . To obtain such a grid, we first generate a n_S -point Halton sequence over $[0, 1]^{d-1}$ then componentwise perform the standard normal quantile transformation $u_j \mapsto z_j := \Phi^{-1}(u_j)$. This yields n_S points $\mathbf{z}_1, \dots, \mathbf{z}_{n_S}$, with

$$\mathbf{z}_j := (\Phi^{-1}(u_{j1}), \dots, \Phi^{-1}(u_{jd})).$$

The resulting unit vectors $\mathbf{z}_j / \|\mathbf{z}_j\|$, $j = 1, \dots, n_S$ constitute the desired sequence over \mathcal{S}^{d-1} .¹⁰

3.2 Factorization of n ((Gi) and (Giii) grids)

As for the grid constructions (Gi) and (Giii), they require a factorization of n into $n_R n_S + n_0$ with $n_0 < \min(n_R, n_S)$. Intuition suggests choosing n_R and n_S of order $n^{1/d}$ and $n^{(d-1)/d}$, respectively. This, however, is of little help for finite n . Since the grid is supposed to provide an approximation of the spherical uniform, we rather proceed by minimizing the Wasserstein distance to the spherical uniform as proposed in Mordant (2021). More precisely, considering the grid with n_R radial points described in (Gi), denote by $G_{n_R}^{(n)}$ the discrete measure placing a probability mass $1/n$ on each of the n gridpoints except for the origin which receives probability mass n_0/n . We adopt here the strategy suggested in Mordant (2021) by selecting the grid with n_R^* radial points, where

$$n_R^* := \arg \min_{1 \leq n_R \leq n} W_2(G_{n_R}^{(n)}, U_d) \quad (4)$$

¹⁰ The justification is the fact that if the distribution of \mathbf{Z} is a product of independent univariate standard normal marginals, then \mathbf{Z} is spherical Gaussian $\mathcal{N}(\mathbf{0}, \mathbf{I})$ and hence $\mathbf{Z}/\|\mathbf{Z}\|$ is uniform over \mathcal{S}^{d-1} .

(W_2 , as usual, stands for the Wasserstein distance of order two). For $d \geq 3$, that distance $W_2(G_{n_R}^{(n)}, U_d)$ does not only depend on n_R (hence on n_S) but also on the n_S points chosen (as explained in Section 3.1) on the hypersphere \mathcal{S}^{d-1} . The minimization in (4) is feasible, as n, n_R, n_S , and n_0 all are integers. A similar strategy is adopted for the construction of the spherical Gaussian grids ((Giii)).

Table 1 provides, for dimensions $d = 2$ and $d = 5$, various sample sizes, and reference distributions the spherical uniform ((Gi) grids) and the spherical Gaussian ((Giii) grids), the “optimal values” obtained via (4) for n_R, n_S , and n_0 . These values are in line with the intuition that the “optimal” n_R behaves like $n^{1/d}$ while the role of distances to the center rapidly decreases as the dimension d increases.

| Reference distribution | d | $n = 50$ | $n = 100$ | $n = 200$ | $n = 300$ | $n = 400$ |
|---|-----|-------------------|--------------------|--------------------|--------------------|--------------------|
| $U_d, (\text{Gi})$ grid | 2 | $n_R = 4$ | $n_R = 6$ | $n_R = 9$ | $n_R = 11$ | $n_R = 12$ |
| | | $n_S = 12$ | $n_S = 16$ | $n_S = 22$ | $n_S = 27$ | $n_S = 33$ |
| | | $n_0 = 2$ | $n_0 = 4$ | $n_0 = 2$ | $n_0 = 3$ | $n_0 = 4$ |
| $\mathcal{N}(\mathbf{0}, \mathbf{I}_d), (\text{Giii})$ grid | 2 | $n_R = 4$ | $n_R = 7$ | $n_R = 11$ | $n_R = 14$ | $n_R = 18$ |
| | | $n_S = 12$ | $n_S = 14$ | $n_S = 18$ | $n_S = 21$ | $n_S = 22$ |
| | | $n_0 = 2$ | $n_0 = 2$ | $n_0 = 2$ | $n_0 = 6$ | $n_0 = 4$ |
| $n^{1/d}$ | | $n^{1/2} = 7.071$ | $n^{1/2} = 10.000$ | $n^{1/2} = 14.142$ | $n^{1/2} = 17.321$ | $n^{1/2} = 20.000$ |
| $U_d, (\text{Gi})$ grid | 5 | $n_R = 2$ | $n_R = 2$ | $n_R = 2$ | $n_R = 3$ | $n_R = 3$ |
| | | $n_S = 25$ | $n_S = 50$ | $n_S = 100$ | $n_S = 100$ | $n_S = 133$ |
| | | $n_0 = 0$ | $n_0 = 0$ | $n_0 = 0$ | $n_0 = 0$ | $n_0 = 1$ |
| $\mathcal{N}(\mathbf{0}, \mathbf{I}_d), (\text{Giii})$ grid | 5 | $n_R = 1$ | $n_R = 1$ | $n_R = 1$ | $n_R = 2$ | $n_R = 2$ |
| | | $n_S = 50$ | $n_S = 100$ | $n_S = 200$ | $n_S = 150$ | $n_S = 200$ |
| | | $n_0 = 0$ | $n_0 = 0$ | $n_0 = 0$ | $n_0 = 0$ | $n_0 = 0$ |
| $n^{1/d}$ | | $n^{1/5} = 2.187$ | $n^{1/5} = 2.512$ | $n^{1/5} = 2.885$ | $n^{1/5} = 3.129$ | $n^{1/5} = 3.314$ |

Table 1 Optimal (in the sense of (4)) values of n_R, n_S , and n_0 as functions of the sample size n , the dimension d , and the reference distributions ((Gi) or (Giii) grids).

3.3 Simulations

Based on the grids obtained along the lines described in Sections 3.1 and 3.2, the distribution-free critical values of the various rank tests under study were computed from 40 000 replications. Throughout, we chose $n_1 = n_2 = n/2$. The optimal maps between the sample and the grids were obtained via an exact solver relying on the so-called Hungarian method that is implemented in the R-package *clue* by Hornik (2021). We now turn to the empirical evaluation of the performance of the various rank-based Wilcoxon and van der Waerden tests for the two-sample location problem.

The objective of our simulations is, essentially, empirical answers to the following two questions:

- should we use spherical grids ((Gi) or (Giii)) or cubic ((Gii) or (Giv)) ones?
- should we, in line with the Hájek tradition, privilege transports to the uniform combined with scores (as in $\left(T_{\text{vdW}\pm}^{(n)}\right)^2$ and $\left(T_{\text{vdW}\square}^{(n)}\right)^2$), or, as recommended by

Deb et al. (2021), should we rather consider “direct transports” to the “scored distribution,” that is, choose as reference distribution the push-forward of the uniform by the score as in $\left(T_{\text{vdW}\pm}^{(n)}\right)^2$ and $\left(T_{\text{vdW}\square}^{(n)}\right)^2$?

4 Wilcoxon-type tests

The Wilcoxon tests are based on the identity score function $\mathbf{J}(\mathbf{u}) = \mathbf{u}$ and uniform (either spherical or cubic) reference distributions, yielding (see Section 2.3.2) the test statistics $\left(T_{\text{W}\pm}^{(n)}\right)^2$ and $\left(T_{\text{W}\square}^{(n)}\right)^2$.

4.1 The bivariate case

In this section, we evaluate the performance of the Wilcoxon tests based on $\left(T_{\text{W}\pm}^{(n)}\right)^2$ and $\left(T_{\text{W}\square}^{(n)}\right)^2$ for samples of size $n_1 = n_2 = n/2$ with $n = 100, 200$, and 400 . The first sample is drawn from a centered distribution, the second one from a shifted version with shift $(\eta, \eta)'$, $\eta > 0$ of the same. The number of replications is $N = 500$.

4.1.1 Spherical Gaussian samples

The first sample is drawn from $\mathcal{N}((0, 0)', \mathbf{I}_2)$, the second one from $\mathcal{N}((\eta, \eta)^\top, \mathbf{I}_2)$ with $\eta > 0$. Rejection frequencies over $N = 500$ replications are shown (as functions of η) in Figure 1. All three tests display, essentially, the same performance: although Wilcoxon, in principle, is strictly less powerful than Hotelling (which in this case is finite-sample optimal), no significant loss of efficiency is detected.

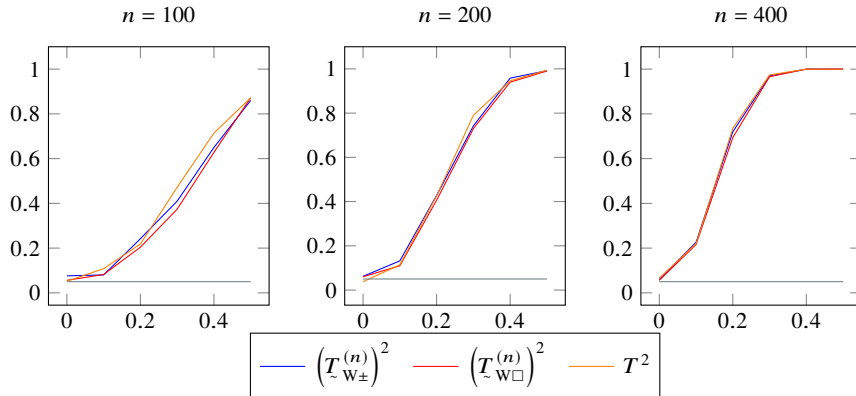


Fig. 1 Rejection frequencies, for spherical Gaussian samples (see 4.4.1) and various sample sizes, of Hotelling’s test based on T^2 and the Wilcoxon tests based on $\left(T_{\text{W}\pm}^{(n)}\right)^2$ and $\left(T_{\text{W}\square}^{(n)}\right)^2$, respectively, as functions of the shift η ; $N = 500$ replications.

4.1.2 Spherical Student samples

The first sample is drawn from a centered spherical Student with 2.1 degrees of freedom $t_{2.1}((0, 0)', \mathbf{I}_2)$, the second one from the shifted version $t_{2.1}((\eta, \eta)', \mathbf{I}_2)$ of the same distribution. Rejection frequencies over $N = 500$ replications are shown (as functions of η) in Figure 2. The Wilcoxon tests substantially outperform Hotelling, an advantage that does not disappear with increasing n . Although the underlying distribution is spherical, very slight superiority of $(T_{W\Box}^{(n)})^2$ over $(T_{W\pm}^{(n)})^2$.

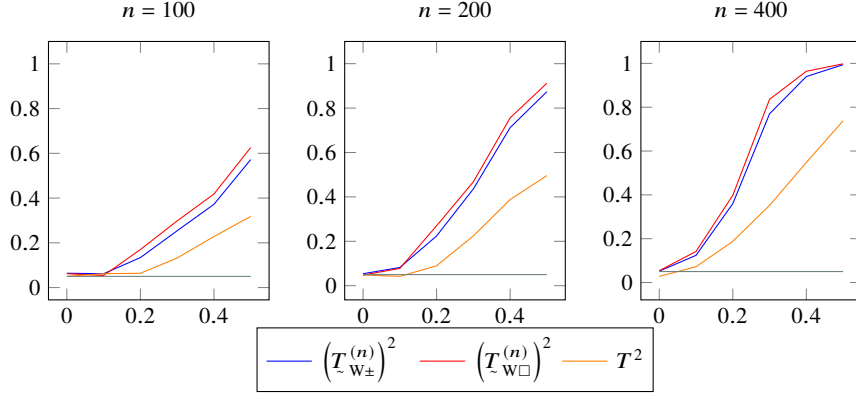


Fig. 2 Rejection frequencies, for Student samples (see 4.1.2) and various sample sizes, of Hotelling's test based on T^2 and the Wilcoxon tests based on $(T_{W\pm}^{(n)})^2$ and $(T_{W\Box}^{(n)})^2$, respectively, as functions of the shift η ; $N = 500$ replications.

4.1.3 “Banana-shaped” samples

The first sample is drawn from a centered “banana-shaped” mixture

$$0.3 \mathcal{N}_2 \left(\begin{pmatrix} 0 \\ -0.7 \end{pmatrix}, \begin{pmatrix} 0.35^2 & 0 \\ 0 & 0.35^2 \end{pmatrix} \right) + 0.35 \mathcal{N}_2 \left(\begin{pmatrix} -0.9 \\ 0.3 \end{pmatrix}, \begin{pmatrix} 0.358 & -0.55 \\ -0.55 & 1.02 \end{pmatrix} \right) \\ + 0.35 \mathcal{N}_2 \left(\begin{pmatrix} 0.9 \\ 0.3 \end{pmatrix}, \begin{pmatrix} 0.358 & 0.55 \\ 0.55 & 1.02 \end{pmatrix} \right).$$

of three Gaussian components. The second sample is drawn from a shifted version (shift $(\eta, \eta)'$, $\eta > 0$) of the same mixture. Rejection frequencies over $N = 500$ replications are shown (as functions of η) in Figure 3. The conclusions are the same as in the previous case, except that the (slight) advantage now belongs to $(T_{W\pm}^{(n)})^2$, despite the fact that the actual distribution is highly nonspherical.

4.1.4 Samples with independent Cauchy marginals

The first sample is drawn from a product of two independent Cauchy, the second one from the shifted version of the same distribution. Rejection frequencies over $N = 500$

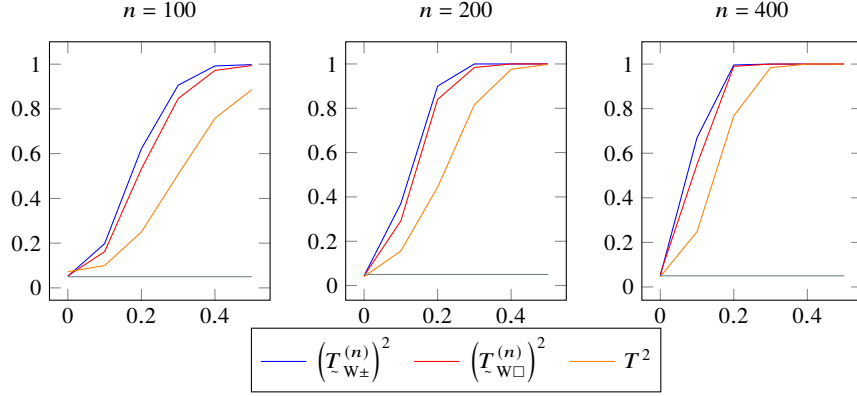


Fig. 3 Rejection frequencies, for “banana-shaped” samples (see 4.1.3) and various sample sizes, of Hotelling’s test based on T^2 and the Wilcoxon tests based on $(T_{W\pm}^{(n)})^2$ and $(T_{W\Box}^{(n)})^2$, respectively, as functions of the shift η ; $N = 500$ replications.

replications are shown (as functions of η) in Figure 4. With a rejection probability uniformly less than the nominal 5% level, Hotelling, as expected, performs miserably. In this independent component situation, $(T_{W\Box}^{(n)})^2$ does outperform $(T_{W\pm}^{(n)})^2$.

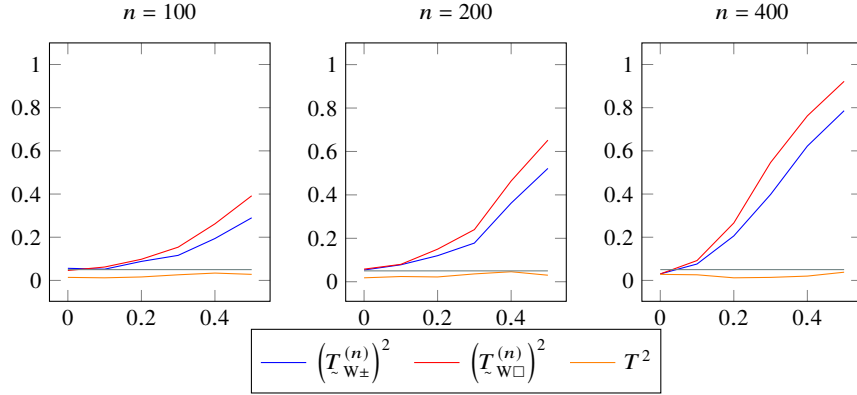


Fig. 4 Rejection frequencies, for samples with independent Cauchy marginals (see 4.1.4) and various sample sizes, of Hotelling’s test based on T^2 and the Wilcoxon tests based on $(T_{W\pm}^{(n)})^2$ and $(T_{W\Box}^{(n)})^2$, respectively, as functions of the shift η ; $N = 500$ replications.

4.1.5 Nonspherical Gaussian samples

The first sample is drawn from a $\mathcal{N}((0,0)', \Sigma)$ distribution, the second sample is drawn from a $\mathcal{N}((\eta, \eta)', \Sigma)$ one; $\text{vech}(\Sigma) = (1, 0.8, 1)'$. Rejection frequencies over $N = 500$ replications are shown (as functions of η) in Figure 5. The results are essentially the same as in the spherical case (Section 4.1.1). Note the loss of power in

the three tests under study, due to the non-specification of the population covariance matrix; that loss, however, is uniform over the three tests.

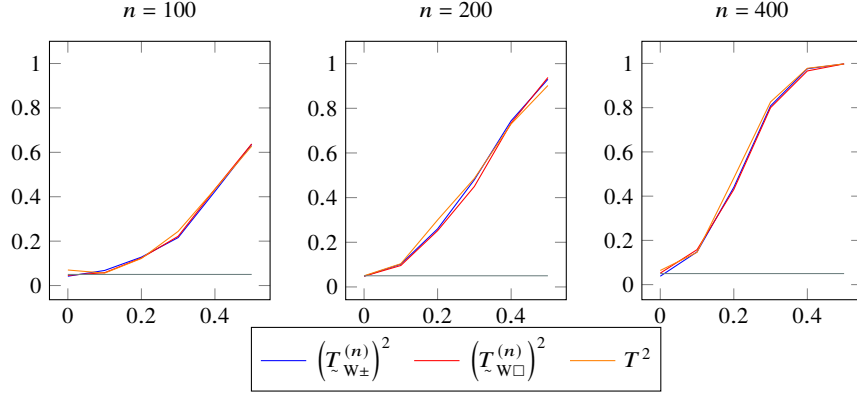


Fig. 5 Rejection frequencies, for samples with nonspherical Gaussian distributions (see 4.1.5) and various sample sizes, of Hotelling's test based on T^2 and the Wilcoxon tests based on $\left(T_{W\pm}^{(n)}\right)^2$ and $\left(T_{W\Box}^{(n)}\right)^2$, respectively, as functions of the shift η ; $N = 500$ replications.

4.1.6 Spherical Cauchy samples

The first sample is drawn from a centered spherical Student with one degree of freedom $t_1((0, 0)', \mathbf{I}_2)$ (spherical Cauchy), the second one from the shifted version $t_1((\eta, \eta)', \mathbf{I}_2)$ of the same distribution. Rejection frequencies over $N = 500$ replications are shown (as functions of η) in Figure 6. The performance of Hotelling, again, is a disaster; although the actual distribution is spherical, $\left(T_{W\Box}^{(n)}\right)^2$ still outperforms $\left(T_{W\pm}^{(n)}\right)^2$.

4.2 Wilcoxon-type statistics in dimension $d = 5$

We essentially adopted the same simulation settings as before, with $n_1 = n_2 = n/2$. A sample size of $n = 100$ in dimension $d = 5$ is very small, though, and we considered sample sizes $n = 200, 400$, and 800 .

4.2.1 Spherical Gaussian samples

Here, the first sample is drawn from the $\mathcal{N}(\mathbf{0}, \mathbf{I}_5)$ distribution, the second one from the $\mathcal{N}(\eta\mathbf{1}, \mathbf{I}_5)$ distribution, where $\mathbf{1}$ denotes a 5-variate vector of ones. Rejection frequencies over $N = 500$ replications are shown (as functions of η) in Figure 7. In the “small sample” case ($n = 200$), the optimality of Hotelling over Wilcoxon is

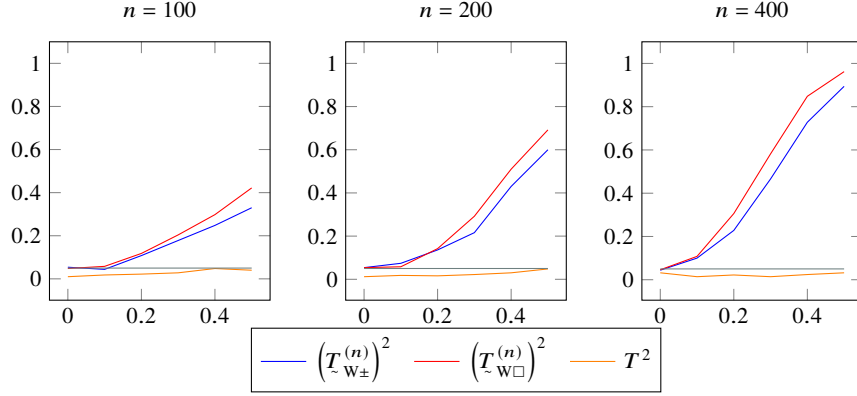


Fig. 6 Rejection frequencies, for samples with spherical Cauchy distributions (see 4.1.6) and various sample sizes, of Hotelling's test based on T^2 and the Wilcoxon tests based on $(T_{W\pm}^{(n)})^2$ and $(T_{W\Box}^{(n)})^2$, respectively, as functions of the shift η ; $N = 500$ replications.

perceptible (more so than in dimension $d = 2$); this superiority, however, fades away with growing n : again, under Gaussian assumptions, abandoning the parametrically optimal Hotelling test in favor of the rank-based Wilcoxon one has no visible cost in terms of power.

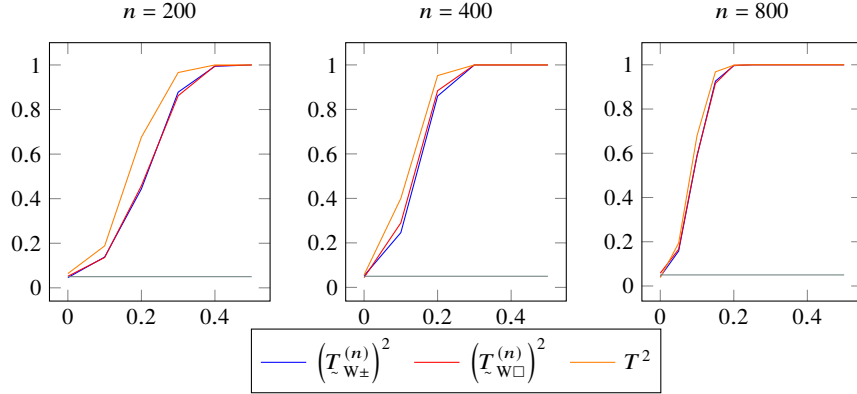


Fig. 7 Rejection frequencies, for samples with 5-dimensional spherical Gaussian distributions (see 4.2.1) and various sample sizes, of Hotelling's test based on T^2 and the Wilcoxon tests based on $(T_{W\pm}^{(n)})^2$ and $(T_{W\Box}^{(n)})^2$, respectively, as functions of the shift η ; $N = 500$ replications.

4.2.2 Spherical Student samples

The first sample is drawn from the centered spherical Student with 2.1 degrees of freedom $t_{2.1}(\mathbf{0}, \mathbf{I}_5)$, the second one from the shifted $t_{2.1}(\eta\mathbf{1}, \mathbf{I}_5)$ distribution, where $\mathbf{1}$ denotes a 5-variate vector of ones. Rejection frequencies over $N = 500$ replications are shown (as functions of η) in Figure 8. The conclusions are quite similar to those

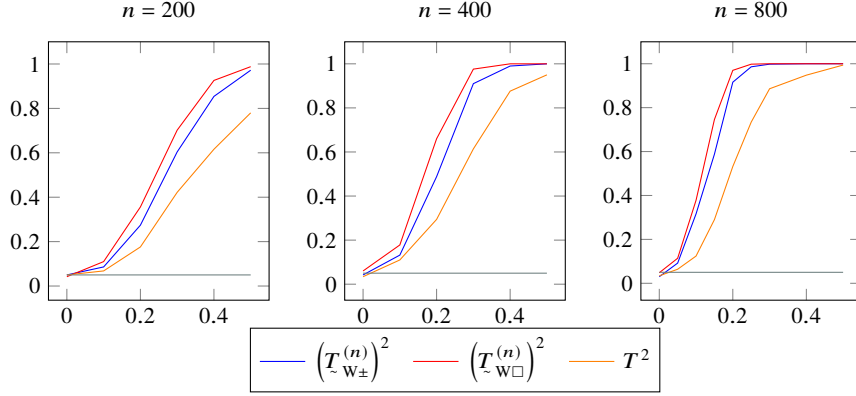


Fig. 8 Rejection frequencies, for samples with 5-dimensional spherical Student $t_{2,1}$ distributions (see 4.2.2) and various sample sizes, of the Wilcoxon tests based on $(T_{W\pm}^{(n)})^2$ and $(T_{W\Box}^{(n)})^2$, respectively, as functions of the shift η ; $N = 500$ replications.

in dimension $d = 2$: although the moments of order two still are finite, the power of Hotelling deteriorates with respect to the Gaussian case. Despite the spherical nature of the actual distribution, slight advantage of $(T_{W\Box}^{(n)})^2$ over $(T_{W\pm}^{(n)})^2$.

4.2.3 Nonspherical Gaussian samples

The first sample is drawn from the $\mathcal{N}(\mathbf{0}, \Sigma)$ distribution, the second one from the $\mathcal{N}(\eta\mathbf{1}, \Sigma)$ distribution, where $\mathbf{1}$ denotes a 5-variate vector of ones and Σ is a correlation matrix with all off-diagonal entries equal to 0.5. Rejection frequencies over $N = 500$ replications are shown (as functions of η) in Figure 9. Here again, the slight advantage of Hotelling over Wilcoxon very rapidly fades away with growing n , and the three tests yield very similar performances; in particular, no significant difference can be detected between $(T_{W\pm}^{(n)})^2$ and $(T_{W\Box}^{(n)})^2$.

4.2.4 Samples with independent Cauchy marginals

The first sample is drawn from a product of five independent Cauchy distributions, the second one from the shifted version of the same. Rejection frequencies over 500 replications are shown (as functions of η) in Figure 10. The performance of Hotelling, as in dimension $d = 2$, is terrible. The advantage (which is in line with the independent component nature of the distribution) of $(T_{W\Box}^{(n)})^2$ over $(T_{W\pm}^{(n)})^2$ is even more significant than in dimension $d = 2$.

5 van der Waerden-type tests

Below we are considering four distinct tests of the van der Waerden type, based (see Section 2.3.2) on $(T_{\text{vdW}\pm}^{(n)})^2$ (spherical uniform reference density, (6i))

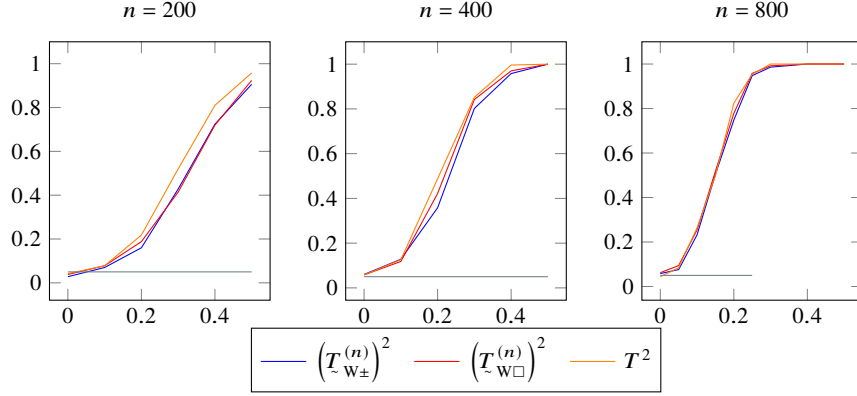


Fig. 9 Rejection frequencies, for nonspherical 5-dimensional Gaussian distributions (see 4.2.3) and various sample sizes, of the Wilcoxon tests based on $(T_{W\pm}^{(n)})^2$ and $(T_{W\Box}^{(n)})^2$, respectively, as functions of the shift η ; $N = 500$ replications. $n = 200$ $n = 400$ $n = 800$

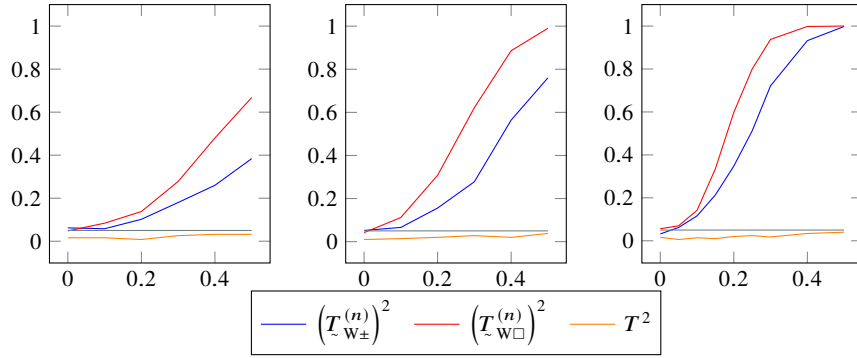


Fig. 10 Rejection frequencies, for 5-dimensional distributions with independent Cauchy marginals (see 4.2.4) and various sample sizes, of Hotelling's test based on T^2 and the Wilcoxon tests based on $(T_{W\pm}^{(n)})^2$ and $(T_{W\Box}^{(n)})^2$, respectively, as functions of the shift η ; $N = 500$ replications.

grid), $(T_{\text{vdW}\Box}^{(n)})^2$ (cubic uniform reference density, (Gii) grid), $(T_{\text{vdW}\pm\mathcal{N}}^{(n)})^2$ (spherical Gaussian reference density, spherical grid (Giii)), and $(T_{\text{vdW}\Box\mathcal{N}}^{(n)})^2$ (spherical Gaussian reference density, cubic grid (Giv)).

5.1 Bivariate case

5.1.1 Spherical Gaussian samples

Same Gaussian samples as in Section 4.1.1. Rejection frequencies over $N = 500$ replications are shown (as functions of η) in Figure 11. Indistinctiveness between the performances of Hotelling and the various rank-based tests is even more pronounced

than for the Wilcoxon tests: definitely, performing rank-based van der Waerden tests does not imply any loss of efficiency in the Gaussian case.

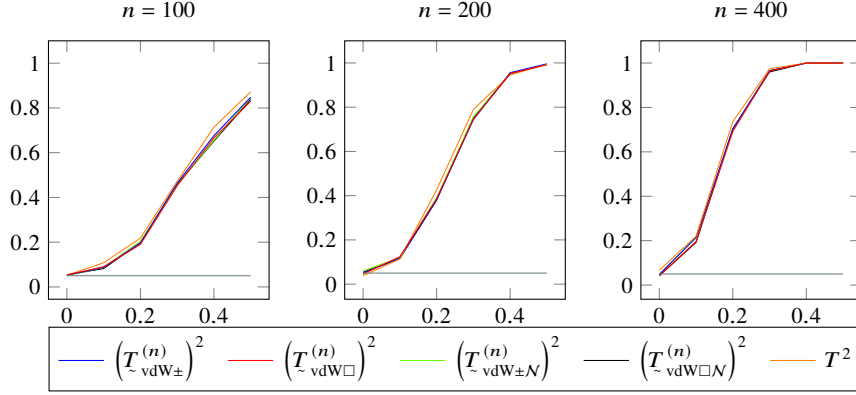


Fig. 11 Rejection frequencies, for spherical Gaussian samples (see 5.1.1) and various sample sizes, of Hotelling's test based on T^2 and the van der Waerden tests based on $(T_{\text{vdW}\pm}^{(n)})^2$, $(T_{\text{vdW}\square}^{(n)})^2$, $(T_{\text{vdW}\pm N}^{(n)})^2$, and $(T_{\text{vdW}\square N}^{(n)})^2$, respectively, as functions of the shift η ; $N = 500$ replications.

5.1.2 Spherical Student samples

Same Student samples as in Section 4.1.2. Rejection frequencies over $N = 500$ replications are shown (as functions of η) in Figure 12. As in dimension $d = 2$, powers are dropping (compared with the Gaussian case). The power of Hotelling, however, deteriorates much more than that of the various versions of van der Waerden tests. The latter all yield very similar performance.

5.1.3 “Banana-shaped” samples

Same “banana-shaped” mixtures as in Section 4.1.3. Rejection frequencies over 500 replications are shown (as functions of η) in Figure 13. The conclusions are quite similar as in the previous case: the empirical power curves of the various van der Waerden tests are essentially indistinguishable, while significantly outperforming the Hotelling ones.

5.1.4 Samples with independent Cauchy marginals

Same samples with independent Cauchy marginals as in Section 4.1.4. Rejection frequencies over $N = 500$ replications are shown (as functions of η) in Figure 14. Again, all powers are much less than in the Gaussian case, but Hotelling is totally inefficient.

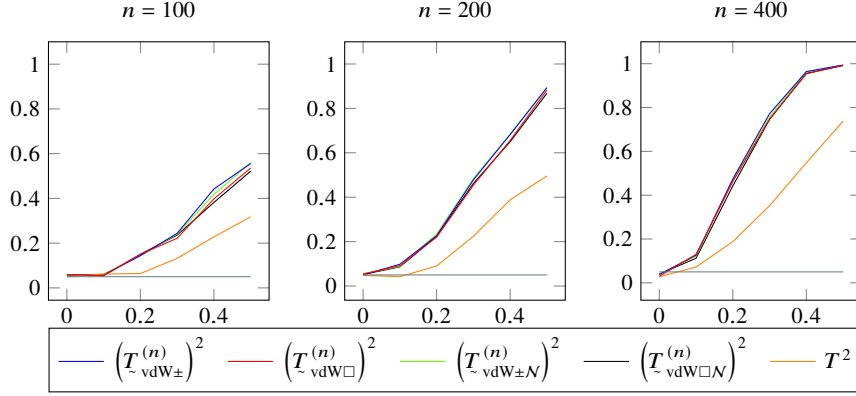


Fig. 12 Rejection frequencies, for spherical Student samples (2.1 degrees of freedom; see 5.1.2) and various sample sizes, of Hotelling's test based on T^2 and the van der Waerden tests based on $(T_{\text{vdW}\pm}^{(n)})^2$, $(T_{\text{vdW}\square}^{(n)})^2$, $(T_{\text{vdW}\pm N}^{(n)})^2$, and $(T_{\text{vdW}\square N}^{(n)})^2$, respectively, as functions of the shift η ; $N = 500$ replications.

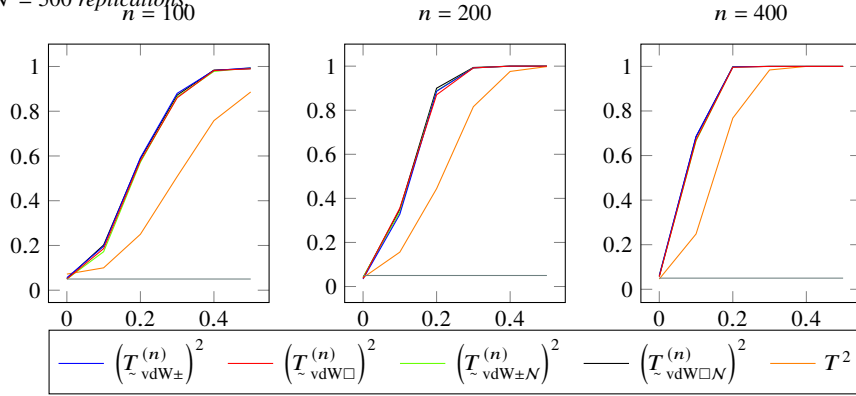


Fig. 13 Rejection frequencies, for "banana-shaped" samples (see Section 5.1.3) and various sample sizes, of Hotelling's test based on T^2 and the van der Waerden tests based on $(T_{\text{vdW}\pm}^{(n)})^2$, $(T_{\text{vdW}\square}^{(n)})^2$, $(T_{\text{vdW}\pm N}^{(n)})^2$, and $(T_{\text{vdW}\square N}^{(n)})^2$, respectively, as functions of the shift η ; $N = 500$ replications.

5.1.5 Nonspherical Gaussian samples

Same correlated Gaussian samples as in Section 4.1.5. Rejection frequencies over $N = 500$ replications are shown (as functions of η) in Figure 15. The non-specification of the covariance matrix apparently has no impact on the comparative performance of Hotelling and its rank-based van der Waerden competitors, which all coincide.

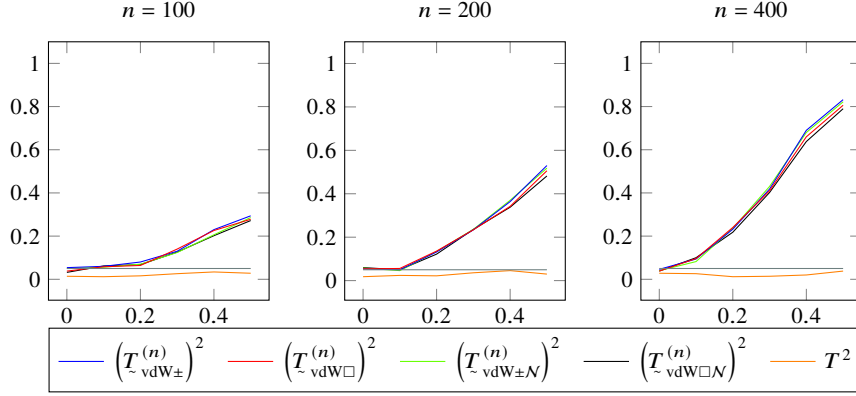


Fig. 14 Rejection frequencies, for samples with independent Cauchy marginals (see Section 5.1.4) and various sample sizes, of Hotelling's test based on T^2 and the van der Waerden tests based on $(T_{\text{vdW}\pm}^{(n)})^2$, $(T_{\text{vdW}\square}^{(n)})^2$, $(T_{\text{vdW}\pm N}^{(n)})^2$, and $(T_{\text{vdW}\square N}^{(n)})^2$, respectively, as functions of the shift η ; $N = 500$ replications.

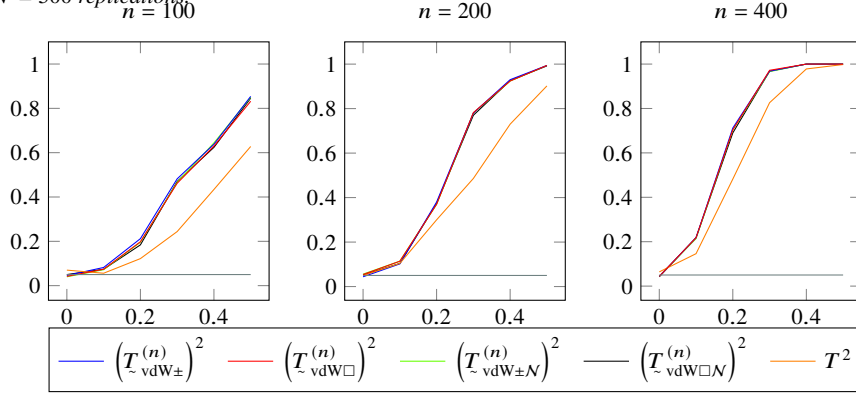


Fig. 15 Rejection frequencies, for nonspherical Gaussian samples (see Section 5.1.5) and various sample sizes, of Hotelling's test based on T^2 and the van der Waerden tests based on $(T_{\text{vdW}\pm}^{(n)})^2$, $(T_{\text{vdW}\square}^{(n)})^2$, $(T_{\text{vdW}\pm N}^{(n)})^2$, and $(T_{\text{vdW}\square N}^{(n)})^2$, respectively, as functions of the shift η ; $N = 500$ replications.

5.1.6 Spherical Cauchy samples

Same spherical Cauchy samples as in Section 4.1.6. Rejection frequencies over 500 replications are shown (as functions of η) in Figure 16. All tests perform similarly except, of course, for Hotelling, which fails completely.

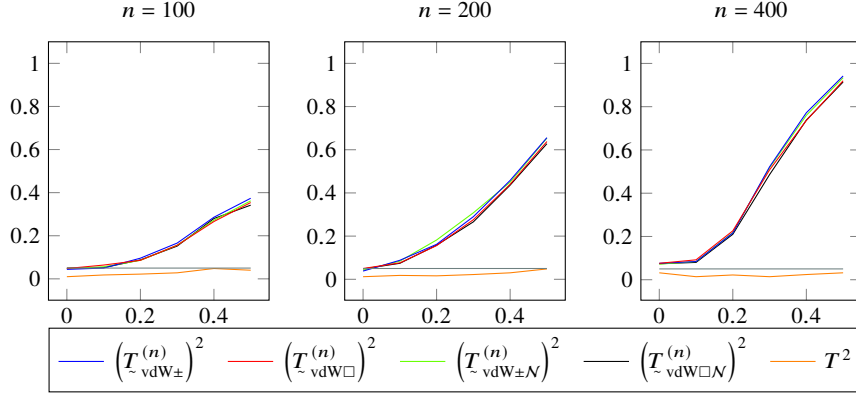


Fig. 16 Rejection frequencies, for spherical Cauchy samples (see Section 5.1.6) and various sample sizes, of Hotelling's test based on T^2 and the van der Waerden tests based on $(T_{\text{vdW}\pm}^{(n)})^2$, $(T_{\text{vdW}\square}^{(n)})^2$, $(T_{\text{vdW}\pm N}^{(n)})^2$, and $(T_{\text{vdW}\square N}^{(n)})^2$, respectively, as functions of the shift η ; $N = 500$ replications.

5.2 van der Waerden-type statistics in dimension $d = 5$

5.2.1 Spherical Gaussian samples

Same spherical Gaussian samples as in Section 4.2.1. Rejection frequencies over $N = 500$ replications are shown (as functions of η) in Figure 17. A “small sample” superiority of Hotelling for $n = 200$ rapidly disappears as n increases; all van der Waerden tests yield the same performance.

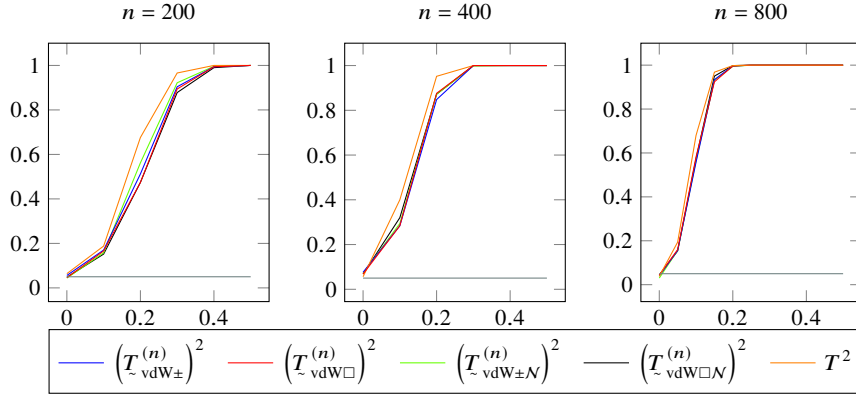


Fig. 17 Rejection frequencies, for samples with 5-dimensional spherical Gaussian distributions (see Section 5.2.1) and various sample sizes, of Hotelling's test based on T^2 and the van der Waerden tests based on $(T_{\text{vdW}\pm}^{(n)})^2$, $(T_{\text{vdW}\square}^{(n)})^2$, $(T_{\text{vdW}\pm N}^{(n)})^2$, and $(T_{\text{vdW}\square N}^{(n)})^2$, respectively, as functions of the shift η ; $N = 500$ replications.

5.2.2 Spherical Student samples

Same spherical Student samples as in Section 4.2.2. Rejection frequencies over 500 replications are shown (as functions of η) in Figure 18. All van der Waerden tests roughly yield the same performance, with a slight advantage in favor of $\left(T_{\text{vdW}\pm\mathcal{N}}^{(n)}\right)^2$ in “small samples.”

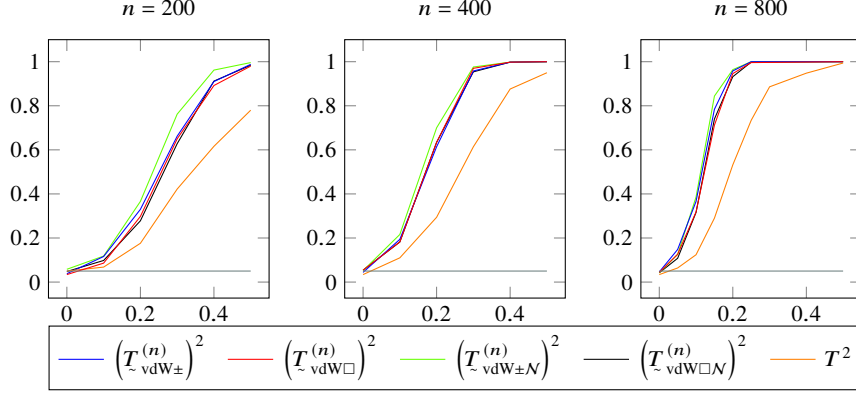


Fig. 18 Rejection frequencies, for samples with 5-dimensional spherical Student distributions (2.1 degrees of freedom; see Section 5.2.2) and various sample sizes, of Hotelling’s test based on T^2 and the van der Waerden tests based on $\left(T_{\text{vdW}\pm}^{(n)}\right)^2$, $\left(T_{\text{vdW}\square}^{(n)}\right)^2$, $\left(T_{\text{vdW}\pm\mathcal{N}}^{(n)}\right)^2$, and $\left(T_{\text{vdW}\square\mathcal{N}}^{(n)}\right)^2$, respectively, as functions of the shift η ; $N = 500$ replications.

5.2.3 Nonspherical Gaussian samples

Same spherical Gaussian samples as in Section 4.2.3. Rejection frequencies over $N = 500$ replications are shown (as functions of η) in Figure 19. The slight advantage for $n = 200$ of Hotelling under spherical Gaussian has almost disappeared. All van der Waerden tests yield similar performance.

5.2.4 Samples with independent Cauchy marginals

Same Cauchy samples as in Section 4.2.4. Rejection frequencies over $N = 500$ replications are shown (as functions of η) in Figure 20. The conclusions drawn for $d = 2$ still hold, with a very slight superiority of the “direct transportation” test $\left(T_{\text{vdW}\pm\mathcal{N}}^{(n)}\right)^2$ over the Gaussian score ones $\left(T_{\text{vdW}\pm}^{(n)}\right)^2$ and $\left(T_{\text{vdW}\square}^{(n)}\right)^2$.

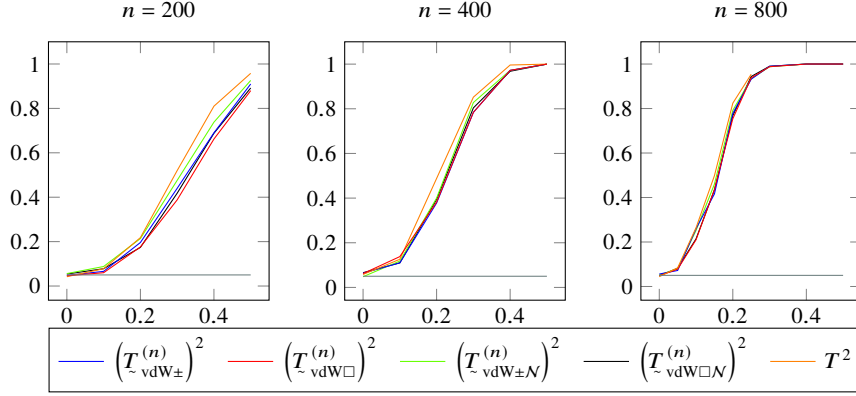


Fig. 19 Rejection frequencies, for nonspherical 5-dimensional Gaussian samples (see Section 5.2.3) and various sample sizes, of Hotelling's test based on T^2 and the van der Waerden tests based on $(T_{\text{vdW}\pm}^{(n)})^2$, $(T_{\text{vdW}\square}^{(n)})^2$, $(T_{\text{vdW}\pm N}^{(n)})^2$, and $(T_{\text{vdW}\square N}^{(n)})^2$, respectively, as functions of the shift η ; $N = 500$ replications.

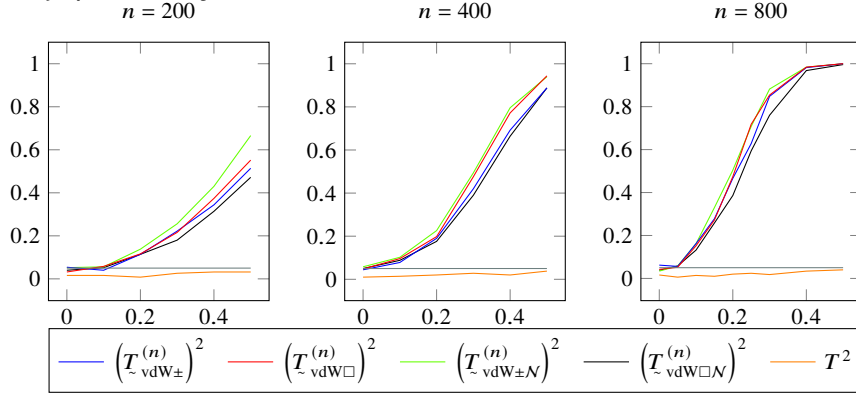


Fig. 20 Rejection frequencies, for 5-dimensional samples with independent Cauchy marginals, (see Section 5.2.4) and various sample sizes, of Hotelling's test based on T^2 and the van der Waerden tests based on $(T_{\text{vdW}\pm}^{(n)})^2$, $(T_{\text{vdW}\square}^{(n)})^2$, $(T_{\text{vdW}\pm N}^{(n)})^2$, and $(T_{\text{vdW}\square N}^{(n)})^2$, respectively, as functions of the shift η ; $N = 500$ replications.

6 Conclusions

While confirming the advantages and excellent performance of rank tests over their daily practice pseudo-Gaussian counterparts, the simulations of the previous sections provide empirical answers to several questions of great practical importance.

The choice of the grid (whether spherical ((G)i), cubic ((G)ii), or Gaussian ((G)iii) and ((G)iv)) seems to have relatively little impact on the performance of the corresponding Wilcoxon tests (the only significant case being the Cauchy one), and no impact at all on the performance of van der Waerden tests. In particular, there is

no evidence that Wilcoxon tests based on spherical grids (G*i*) are preferable under spherical distributions while Wilcoxon tests based on cubic grids (G*ii*) are preferable under distributions with independent components: see, e.g., the Cauchy case (Sections 4.1.6 and 4.1.4).

References

- Carlier, G., Chernozhukov, V., & Galichon, A. (2016). Vector quantile regression: an optimal transport approach. *Ann. Statist.*, *44*, 1165–92.
URL <https://doi.org/10.1214/15-AOS1401>
- Chernozhukov, V., Galichon, A., Hallin, M., & Henry, M. (2017). Monge-Kantorovich depth, quantiles, ranks and signs. *Ann. Statist.*, *45*, 223–256.
URL <https://doi.org/10.1214/16-AOS1450>
- Deb, N., Bhattacharya, B. B., & Sen, B. (2021). Efficiency lower bounds for distribution-free Hotelling-type two-sample tests based on optimal transport. ArXiv:2104.01986.
- Deb, N., Ghosal, P., & Sen, B. (2020). Measuring association on topological spaces using kernels and geometric graphs. ArXiv:2010.01768.
- Deb, N., & Sen, B. (2021). Multivariate rank-based distribution-free nonparametric testing using measure transportation. *Journal of the American Statistical Association*, *0*(0), 1–16.
URL <https://doi.org/10.1080/01621459.2021.1923508>
- del Barrio, E., González-Sanz, A., & Hallin, M. (2020). A note on the regularity of optimal-transport-based center-outward distribution and quantile functions. *J. Multivariate Anal.*, *180*, 104671, 13.
URL <https://doi.org/10.1016/j.jmva.2020.104671>
- Faugeras, O., & Rüschendorf, L. (2017). Markov morphisms: a combined copula and mass transportation approach to multivariate quantiles. *Mathematica Applicanda*, *45*, 21–63.
- Figalli, A. (2018). On the continuity of center-outward distribution and quantile functions. *Non-linear Anal.*, *177*, 413–21.
URL <https://doi.org/10.1016/j.na.2018.05.008>
- Ghosal, P., & Sen, B. (2019). Multivariate ranks and quantiles using optimal transportation and applications to goodness-of-fit testing. ArXiv:1905.05340.
- Hájek, J., & Šidák, Z. (1967). *Theory of Rank Tests*. Academic Press, New York.
- Hallin, M. (2017). On distribution and quantile functions, ranks, and signs in \mathbb{R}^d : a measure transportation approach. ideas.repec.org/p/eca/wpaper/2013-258262.html.
- Hallin, M. (2022). Measure transportation and statistical decision theory. *Annual Review of Statistics and its Applications*, in press, 9.
URL <https://doi.org/10.1146/annurev-statistics-040220-105948>
- Hallin, M., Del Barrio, E., Cuesta-Albertos, J., & Matrán, C. (2021). Distribution and quantile functions, ranks and signs in dimension d : A measure transportation approach. *The Annals of Statistics*, *49*, 1139–1165.
- Hallin, M., Hlubinka, D., & Hudecová, Š. (2020a). Fully distribution-free center-outward rank tests for multiple-output regression and MANOVA. ArXiv:2007.15496.
- Hallin, M., La Vecchia, D., & Liu, H. (2020b). Center-outward R-estimation for semiparametric VARMA models. *Journal of the American Statistical Association*, in press.
URL <https://doi.org/10.1080/01621459.2020.1832501>
- Hallin, M., La Vecchia, D., & Liu, H. (2020c). Rank-based testing for semiparametric var models: a measure transportation approach. ArXiv:2011.06062.
- Hallin, M., & Paindaveine, D. (2002). Optimal tests for multivariate location based on interdirections and pseudo-Mahalanobis ranks. *Ann. Statist.*, *30*, 1103–33.

- Hampel, F. R. (1968). *Contributions to the Theory of Robust Estimation*. Ph.D. thesis, University of California, Berkeley.
- Hornik, K. (2021). *clue: Cluster ensembles*. R package version 0.3-60.
URL <https://CRAN.R-project.org/package=clue>
- Huber, P. (1964). Robust estimation of a location parameter. *Annals of Mathematical Statistics*, 35, 73–101.
- Masud, S. B., & Aeron, S. (2021). Soft and subspace robust multivariate rank tests based on entropy regularized optimal transport. ArXiv:2103.08811.
- McCann, R. J. (1995). Existence and uniqueness of monotone measure-preserving maps. *Duke Math. J.*, 80, 309–324.
- McDonald, T., & McDonald, A. (2020). *SDraw: Spatially balanced samples of spatial objects*. R package version 2.1.13.
URL <https://CRAN.R-project.org/package=SDraw>
- Mordant, G. (2021). *Transporting Probability Measures: some contributions to statistical inference*. Ph.D. thesis, Université catholique de Louvain.
- Ronchetti, E. (2006). The historical development of robust statistics. In A. Rossman, & B. Chance (Eds.) *ICOTS-7 Proceedings*. IASE.
- Shi, H., Drton, M., & Han, F. (2021a). Distribution-free consistent independence tests via center-outward ranks and signs. *Journal of the American Statistical Association*, in press.
- Shi, H., Hallin, M., Drton, M., & Han, F. (2021b). On universally consistent and fully distribution-free rank tests of vector independence. *Annals of Statistics*, to appear.
- Stigler, S. M. (1973). Simon Newcomb, Percy Daniell, and the history of robust estimation 1885–1920. *Journal of the American Statistical Association*, 68, 872–879.
- Tukey, J. W. (1960). A survey of sampling from contaminated distributions. In I. Olkin (Ed.) *Contributions to Probability and Statistics*, (pp. 448–485). Palo Alto: Stanford University Press.